10.24425/acs.2025.157141

Archives of Control Sciences
Volume 35(LXXI), 2025
No. 4, *pages* 635–653

A novel 5D hyperchaotic system with multi-layer attractors: sliding mode control and electronic circuit implementation

Manal MECHEKEF and Lotfi MEDDOUR

This paper introduces a novel 5D hyperchaotic system derived from a 3D chaotic system. The system has a unique equilibrium point at the origin and exhibits two positive Lyapunov exponents, demonstrating a complex multi-layer attractor structure. Its rich dynamical behavior suggests strong potential for applications in secure communications and control systems engineering. In line with these capabilities, we propose a sliding mode control strategy to stabilize the system at the origin. The designed controllers drive system states toward a predefined sliding surface and maintain them there, with convergence and stability rigorously proven using Lyapunov theory. Furthermore, we realize the system as an electronic circuit in Multisim and verify its hyperchaotic behavior through phase portrait analysis in MATLAB.

Key words: hyperchaotic system, Lyapunov exponents, sliding mode control, electronic circuit

1. Introduction

Since the discovery of the Lorenz model in 1963 as a 3D chaotic system that exhibits sensitivity to initial conditions [1], research in this field has accelerated. Over time, researchers have introduced new chaotic systems that exhibit complex dynamics and distinct topological properties, such as [2–8], although some studies have demonstrated the equivalence of certain systems to the Lorenz model, such as the Chen model [9, 10]. The rapid development of chaotic systems has led to the emergence of hyperchaotic systems. Hyperchaos is a complex dynamical

M. Mechekef (e-mail: manal.mechekef@doc.umc.edu.dz) is with Laboratory of Applied Mathematics and Modeling, Faculty of Exact Sciences, University of Constantine 1, Constantine, 25017, Algeria.

L. Meddour (corresponding author, e-mail: Meddour_lotfi@umc.edu.dz) is with Laboratory of Mathematical Modeling and Simulation, Faculty of Exact Sciences, University of Constantine 1, Constantine, 25017, Algeria.

Received 04.05.2025. Revised 26.08.2025.

behavior typically described as an advanced form of a chaotic system that can be extended and adapted to higher-dimensional systems. While chaotic systems exhibit sensitivity to initial conditions, exponential trajectory divergence, and a single positive Lyapunov exponent, hyperchaotic systems are characterized by the presence of more than one positive Lyapunov exponent and require at least four dimensions. This means that hyperchaotic systems exhibit exponential divergence of trajectories in multiple directions, making their behavior even more unpredictable and intricate than that of chaotic systems.

The concept of hyperchaos was first introduced by Otto Rössler in 1979 [11], when he discovered a four-dimensional system by extending his three-dimensional chaotic system into four dimensions. This system, later named the Rössler hyperchaotic system, marked the beginning of the study of hyperchaos. Since then, numerous hyperchaotic systems have been developed, including the hyperchaotic Lorenz system, the hyperchaotic Chen system, the hyperchaotic Chua's circuit, the hyperchaotic Lü system, and many others [12–20]. Due to their complex properties, hyperchaotic systems are widely studied in various scientific and engineering domains, especially in areas requiring high unpredictability and complex signal generation, such as secure communication, cryptography, random number generation, biological system modeling, and electronic circuits [21–25]. Among the various classes of hyperchaotic systems, five-dimensional hyperchaotic systems represent a significant and increasingly studied category because of their greater complexity and richer bifurcation structures. Additionally, due to the intrinsic sensitivity and unpredictability of hyperchaotic systems, controlling their behavior becomes a crucial task, particularly for ensuring stable operation or synchronization.

The study of hyperchaotic system control focuses on developing feedback control strategies to achieve global or local asymptotic stabilization and regulate system outputs, this is essential for enhancing stability and performance across diverse fields, including engineering, medicine, economics, and communications. Several approaches have been developed for controlling hyperchaotic systems, such as active control [17, 26, 27], which directly modifies the system equations; adaptive control [16, 28, 29], which is effective for systems with unknown parameters; and sliding mode control [30–35], which provides robustness against uncertainties and external disturbances, fast response, and relatively simple implementation once the sliding surface is defined, among others. To take advantage of the above, hyperchaotic systems can be represented using controlled electrical circuits, which serve as a low-cost and highly efficient solution for encrypted communications, random number generation, bio-signal analysis, intelligent systems, and noise filtering, especially for nonlinear or very weak signals [36–43]. The biggest challenge lies in designing the optimal circuit,

but with modern simulation tools, achieving this with precision has become feasible.

This paper is structured as follows: Section 2 introduces a novel 5D hyperchaotic system with four nonlinear equations and analyzes its complexity by examining its equilibrium points, stability, bifurcation diagrams, Lyapunov exponents, as well as visualizing its attractor using MATLAB. In Section 3, sliding mode control is proposed to ensure the stability of the hyperchaotic system by designing an exponential reaching law to force the system states to reach and remain on the sliding surface, with stability established using Lyapunov theory. The SMC approach has been chosen due to its effective for controlling nonlinear systems, especially in chaotic and hyperchaotic systems. Due to its simple design, which makes its application easy compared to other methods. It also ensures global asymptotic stability of the system and is characterized by its robustness against uncertainties and external disturbances. In Section 4, the hyperchaotic system is implemented in an electronic circuit using Multisim to validate the theoretical findings, demonstrating its practical feasibility. Finally, a brief conclusion is provided in Section 5.

2. Formulation and Dynamic Analysis of a 5D Hyperchaotic System

2.1. Construction of a New Hyperchaotic System

The generalized Lorenz system family [44] is characterized by the following dynamics:

$$\begin{cases} \dot{x} = a(y - x), \\ \dot{y} = cx + dy - xz, \\ \dot{z} = xy - ez. \end{cases} \tag{1}$$

Through state feedback control of system (1), we develop a new nonlinear system described by:

$$\begin{cases} \dot{x} = a(y - x) + bu, \\ \dot{y} = cx + dy - xz + v, \\ \dot{z} = xy - ez, \\ \dot{u} = -mx - my^3, \\ \dot{v} = -nyz, \end{cases} \tag{2}$$

where x, y, z, u, and v are state variables, and a, b, c, d, e, m, $n \in \mathbb{R}$ are constant parameters.

For parameter values $a = 1$, $b = 7$, $c = 9$, $d = 2$, $e = 6$, $m = 3$, and $n = 7$, the system (2) exhibits hyperchaotic behavior with two positive Lyapunov exponents,

as shown in Fig. 1. The Lyapunov exponents are:

$$L_1 = 3.300219, \quad L_2 = 0.163290, \quad L_3 = -0.062670,$$

$$L_4 = -2.231652, \quad \text{and} \quad L_5 = -6.170517,$$

satisfying:

$$\sum_{i=1}^{5} L_i < 0.$$

The Kaplan-Yorke dimension is given by:

$$D_{KY} = j + \frac{\sum_{i=1}^{j} L_i}{|L_{j+1}|} = 4 + \frac{L_1 + L_2 + L_3 + L_4}{|L_5|} = 4.189479.$$

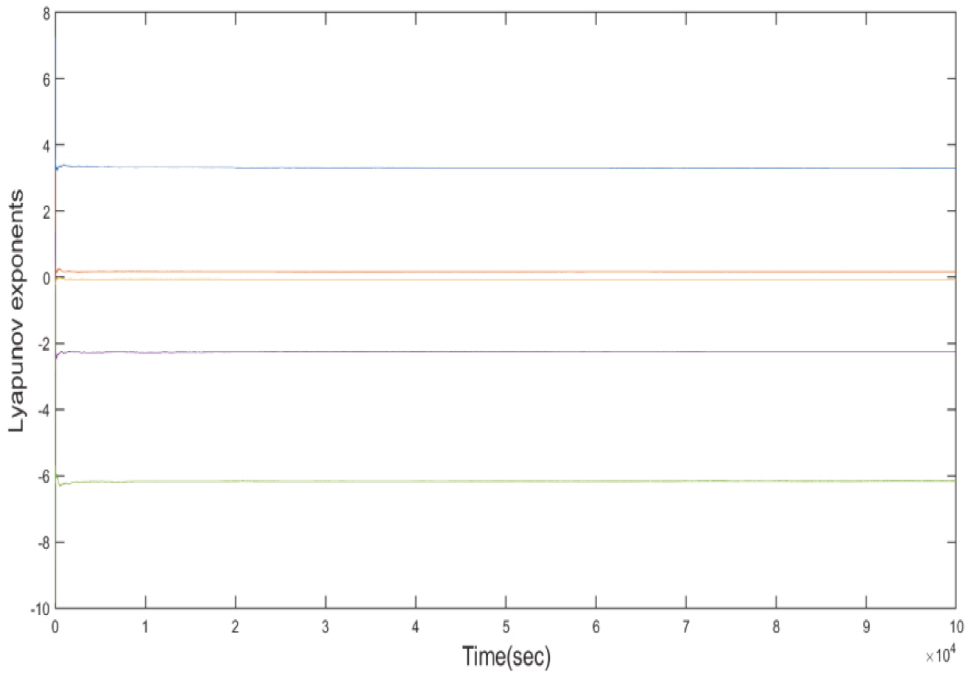

Figure 1: Time evolution of Lyapunov exponents of the system (2) with parameters $a = 1$, $b = 7$, $c = 9$, $d = 2$, $e = 6$, $m = 3$, and $n = 7$

The phase portraits of the system (2) across different planes, illustrating its complex multi-layer attractor structure, are shown in Fig. 2.

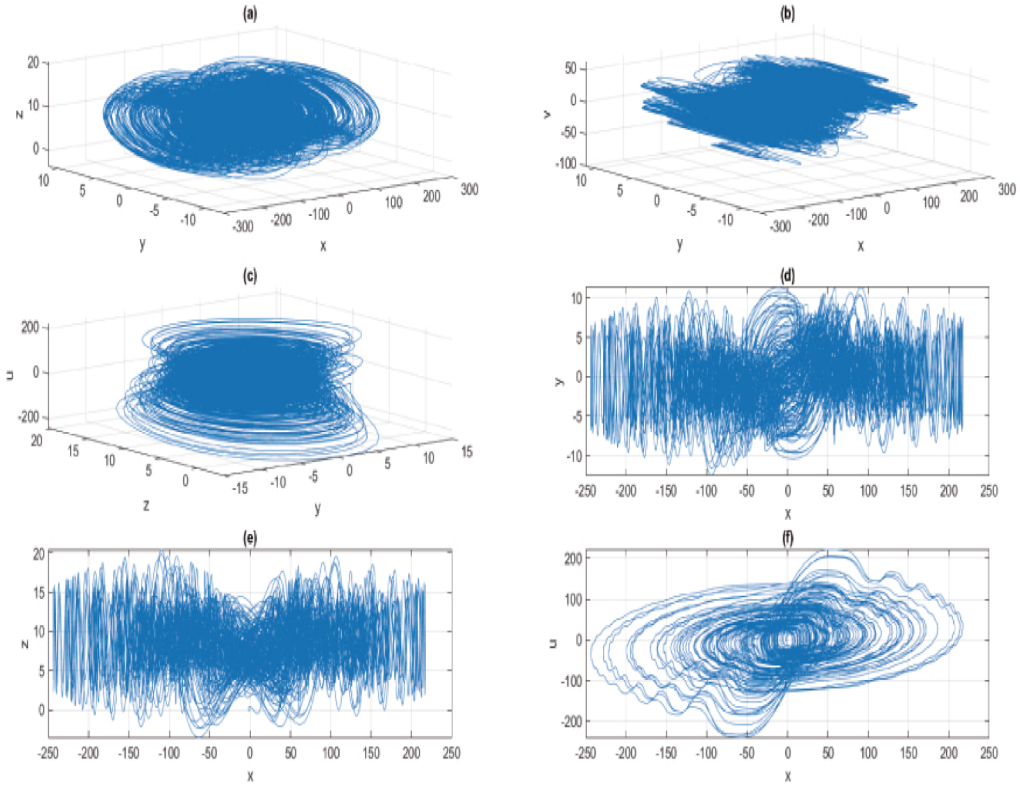

Figure 2: Phase portraits of the hyperchaotic system (2) in (a) $x-y-z$ space; (b) $x-y-v$ space; (c) $y-z-u$ space; (d) $x-y$ plane; (e) $x-z$ plane; (f) $x-u$ plane, with parameters $a = 1, b = 7, c = 9, d = 2, e = 6, m = 3, n = 7$, and initial conditions $(x_0, y_0, z_0, u_0, v_0) = (0.1, 0.1, 0.1, 0.1, 0.1)$

2.2. Symmetry and invariance

The system (2) exhibits invariance under the transformation $(x, y, z, u, v) \rightarrow (-x, -y, z, -u, -v)$, which represents a reflection across the z-axis. This symmetry means that the system's behavior remains unchanged when the x, y, u, and v coordinates are inverted, while the z coordinate remains unchanged. In summary, for every trajectory in the system, there exists a corresponding symmetric trajectory, reflecting the system's inherent structural invariance.

2.3. Dissipativity

The divergence of the novel system (2) is given by:

$$\nabla \mathbf{V} = \frac{\partial \dot{x}}{\partial x} + \frac{\partial \dot{y}}{\partial y} + \frac{\partial \dot{z}}{\partial z} + \frac{\partial \dot{u}}{\partial u} + \frac{\partial \dot{v}}{\partial v} = -(a - d + e). \tag{3}$$

Thus, system (2) is dissipative when $(a - d + e) > 0$. It exhibits exponential contraction at a rate of $\exp(-(a - d + e))$, converging to zero as $t \to \infty$. Consequently, the system's asymptotic behavior settles onto an attractor.

2.4. Equilibria and stability

The system (2) has a unique equilibrium point $E_0 = (0, 0, 0, 0, 0)$, which can be calculated by setting $\dot{x} = \dot{y} = \dot{z} = \dot{u} = \dot{v} = 0$.

The stability of the equilibrium E_0 can be studied by calculating the Jacobian matrix (4), which is given by:

$$J_{E_0} = \begin{pmatrix} -a & a & 0 & b & 0 \\ c & d & 0 & 0 & 1 \\ 0 & 0 & -e & 0 & 0 \\ -m & 0 & 0 & 0 & 0 \\ 0 & 0 & 0 & 0 & 0 \end{pmatrix}. \tag{4}$$

The characteristic polynomial of the Jacobian matrix given in (4) is:

$$\Delta(\lambda) = \lambda(\lambda + e)(-\lambda^3 + (-a + d)\lambda^2 + (ad + ac + bm)\lambda - bm). \tag{5}$$

The eigenvalues are obtained by solving the characteristic equation $\Delta(\lambda) = 0$, which yields:

$$\lambda_1 = 0, \quad \lambda_2 = -e, \quad -\lambda^3 + (-a + d)\lambda^2 + (ad + ac + bm)\lambda - bm = 0.$$

According to the Routh-Hurwitz stability criterion, all eigenvalues have negative real parts if and only if the following conditions are satisfied:

$$a > d, \quad bm > 0, \quad \text{and} \quad bm < (-a + d)(ad + ac + bm). \tag{6}$$

The equilibrium point E_0 is stable when $e > 0$ and conditions (6) are satisfied.

2.5. Bifurcation and Poincaré section

The bifurcation diagram of system (2) for parameter $n \in [0, 30]$, as shown in Fig. 3, exhibits rich and complex dynamical behavior. This diagram was computed with fixed parameters $a = 1$, $b = 7$, $c = 9$, $d = 2$, $e = 6$, $m = 3$, and initial conditions $(x_0, y_0, z_0, u_0, v_0) = (0.1, 0.1, 0.1, 0.1, 0.1)$.

Furthermore, we analyze the Poincaré map of system (2). As shown in Fig. 4, the Poincaré sections consist of scattered points, confirming the chaotic behavior of the system.

The combined theoretical analysis and numerical simulations confirm that the novel hyperchaotic system (2) exhibits both complex topological structures and diverse chaotic dynamics.

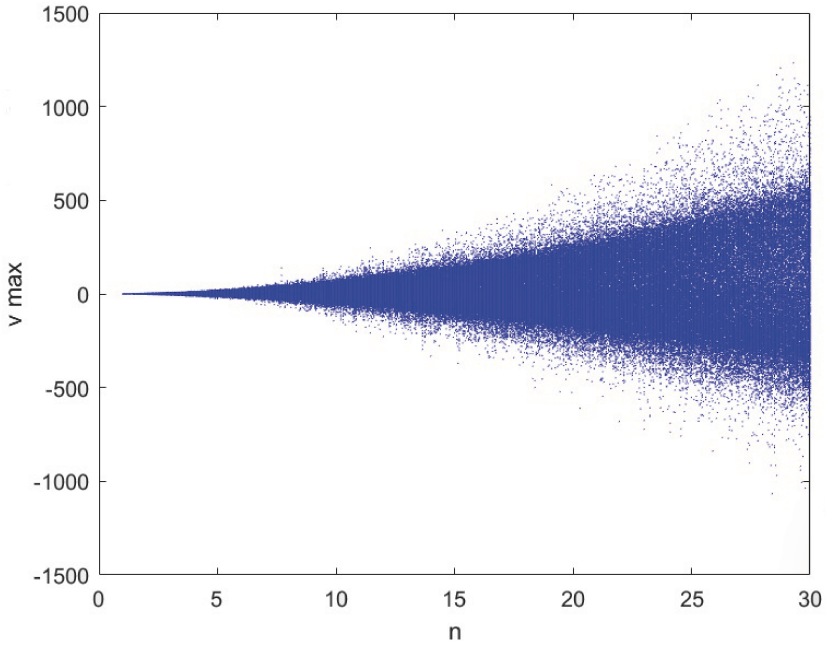

Figure 3: Bifurcation diagram of system (2) with respect to parameter n, for fixed parameters $a = 1$, $b = 7$, $c = 9$, $d = 2$, $e = 6$, $m = 3$, and initial conditions $(x_0, y_0, z_0, u_0, v_0) = (0.1, 0.1, 0.1, 0.1, 0.1)$

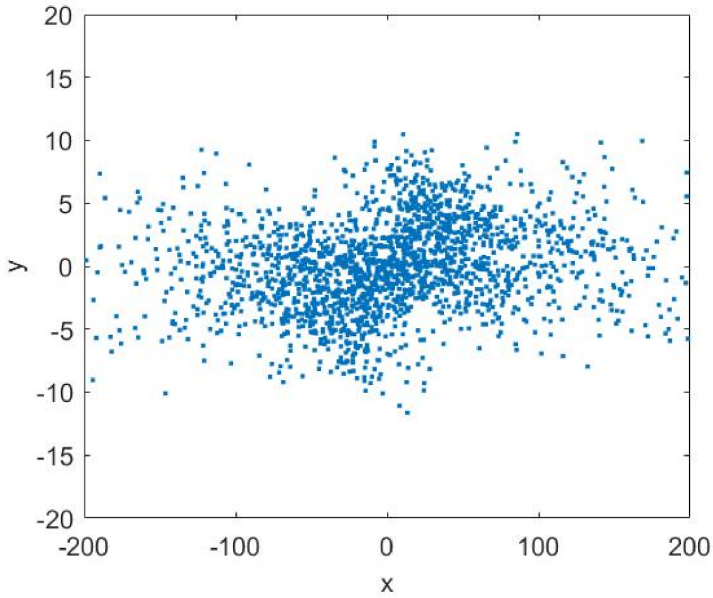

Figure 4: The Poincaré map of the system (2) on the $x - y$ plane

3. Sliding mode control design for the novel 5D hyperchaotic system

In this section, a sliding mode control strategy is applied to drive the system state trajectories toward the sliding surface, achieving global stabilization of the hyperchaotic dynamics.

The controlled hyperchaotic system is described as follows:

$$\begin{cases} \dot{x} = a(y-x) + bu + \mu_x\,, \\ \dot{y} = cx + dy - xz + v + \mu_y\,, \\ \dot{z} = xy - ez + \mu_z\,, \\ \dot{u} = -mx - my^3 + \mu_u\,, \\ \dot{v} = -nyz + \mu_v\,, \end{cases} \tag{7}$$

where μ_i (for $i = x, y, z, u, v$) are feedback controllers that should be designed based on the system variables x, y, z, u, v such that the system in equations (7) globally converges to the origin asymptotically.

To ensure the asymptotic stability of the sliding mode, a suitable sliding surface in this design is described as follows:

$$\begin{cases} S_x = x + \lambda_x \displaystyle\int_0^t x(\tau)\,\mathrm{d}\tau, \\ S_y = y + \lambda_y \displaystyle\int_0^t y(\tau)\,\mathrm{d}\tau, \\ S_z = z + \lambda_z \displaystyle\int_0^t z(\tau)\,\mathrm{d}\tau, \\ S_u = u + \lambda_u \displaystyle\int_0^t u(\tau)\,\mathrm{d}\tau, \\ S_v = v + \lambda_v \displaystyle\int_0^t v(\tau)\,\mathrm{d}\tau, \end{cases} \tag{8}$$

where λ_i (for $i = x, y, z, u, v$) are positive constants chosen by the designer.

The derivative of the sliding surface (8) is given as follows:

$$\begin{cases} \dot{S}_x = \dot{x} + \lambda_x x, \\ \dot{S}_y = \dot{y} + \lambda_y y, \\ \dot{S}_z = \dot{z} + \lambda_z z, \\ \dot{S}_u = \dot{u} + \lambda_u u, \\ \dot{S}_v = \dot{v} + \lambda_v v. \end{cases} \tag{9}$$

The control law is presented as follows:

$$\mu_i = \mu_{e_i} + \mu_{d_i}\,, \tag{10}$$

where $i \in \{x, y, z, u, v\}$ and μ_{ei} is the equivalent controller, calculated using the invariance condition, allowing us to cancel out the known terms on the right-hand side of (9). It is determined using the exponential reaching law for $i \in \{x, y, z, u, v\}$, given as follows:

$$\begin{aligned} S_i > 0 \;&\Rightarrow\; \dot{S}_i < 0, \\ S_i < 0 \;&\Rightarrow\; \dot{S}_i > 0, \end{aligned}$$

which must satisfy two conditions:

$$Si = 0 \quad \text{and} \quad \dot{S}_i = -\eta_i \text{sign}(S_i) - k_i S_i\,. \tag{11}$$

By using the condition (11) in (8) and substituting (7) into (9), the equivalent controller is given as:

$$\begin{cases} \mu_{e_x} = -a(y - x) - bu - \lambda_x x, \\ \mu_{e_y} = -cx - dy + xz + v - \lambda_y y, \\ \mu_{e_z} = -xy + ez - \lambda_z z, \\ \mu_{e_u} = mx + my^3 - \lambda_u u, \\ \mu_{e_v} = nyz - \lambda_v v. \end{cases} \tag{12}$$

And μ_{d_i} for $i \in \{x, y, z, u, v\}$ is defined as an external discontinuous control effort that forces the system to ensure finite-time convergence to the sliding surface. Under condition (11), the controller μ_{di} is chosen as:

$$\mu_{d_i} = -\eta_i \text{sign}(S_i) - k_i S_i, \tag{13}$$

where η_i and k_i are positive constants. Substituting (12) and (13) into (10), the controller is obtained:

$$\begin{cases} \mu_x = -a(y-x) - bu - \lambda_x x - \eta_x \text{sign}(S_x) - k_x S_x \,, \\ \mu_y = -cx - dy + xz - v - \lambda_y y - \eta_y \text{sign}(S_y) - k_y S_y \,, \\ \mu_z = -xy + ez - \lambda_z z - \eta_z \text{sign}(S_z) - k_z S_z \,, \\ \mu_u = mx + my^3 - \lambda_u u - \eta_u \text{sign}(S_u) - k_u S_u \,, \\ \mu_v = nyz - \lambda_v v - \eta_v \text{sign}(S_v) - k_v S_v \,. \end{cases} \tag{14}$$

Theorem 1. *Consider the system (7) with the initial condition values $x(0)$, $y(0)$, $z(0)$, $u(0)$, $v(0) \in \mathbb{R}$. Under the proposed sliding mode controller (14), the origin is globally asymptotically stable if the design parameters satisfy: $\lambda_i > 0$, $\eta_i > 0$, $k_i > 0$, for $i \in \{x, y, z, u, v\}$.*

Proof. Let the Lyapunov function of the system be defined as:

$$V = \frac{1}{2}\left(S_x^2 + S_y^2 + S_z^2 + S_u^2 + S_v^2\right). \tag{15}$$

Clearly, $V \geqslant 0$ and $V = 0$ if and only if $S_x = S_y = S_z = S_u = S_v = 0$. Thus, V is positive definite and radially unbounded.

Differentiating V along the system trajectories yields:

$$\begin{aligned} \dot{V} &= S_x\dot{S}_x + S_y\dot{S}_y + S_z\dot{S}_z + S_u\dot{S}_u + S_v\dot{S}_v \\ &= S_x(-\eta_x \text{sign}(S_x) - k_x S_x) + S_y(-\eta_y \text{sign}(S_y) - k_y S_y) \\ &\quad + S_z(-\eta_z \text{sign}(S_z) - k_z S_z) + S_u(-\eta_u \text{sign}(S_u) - k_u S_u) \\ &\quad + S_v(-\eta_v \text{sign}(S_v) - k_v S_v) \\ &= -\eta_x|S_x| - k_x S_x^2 - \eta_y|S_y| - k_y S_y^2 - \eta_z|S_z| - k_z S_z^2 - \eta_u|S_u| - k_u S_u^2 \\ &\quad - \eta_v|S_v| - k_v S_v^2 \,. \end{aligned}$$

Since $\eta_i > 0$ and $k_i > 0$ for all $i \in \{x, y, z, u, v\}$, it follows that $\dot{V} < 0$ for all $S_i \neq 0$, and $\dot{V} = 0$ only when $S_i = 0$. Therefore, by Lyapunov's direct method, the system trajectories converge asymptotically to the sliding surface $S_i = 0$.

On the sliding surface, $S_i = 0$ implies:

$$\dot{x} + \lambda_x x = 0, \quad \dot{y} + \lambda_y y = 0, \quad \dot{z} + \lambda_z z = 0, \quad \dot{u} + \lambda_u u = 0, \quad \dot{v} + \lambda_v v = 0.$$

These are first-order linear systems with solutions:

$$x(t) = x(0)e^{-\lambda_x t}, \quad y(t) = y(0)e^{-\lambda_y t}, \quad \ldots$$

Since $\lambda_i > 0$ for all $i \in \{x, y, z, u, v\}$, all states converge to zero as $t \to \infty$.

Hence, the system (7) is globally asymptotically stable at the origin. □

In the simulation results, Python is used to solve the proposed hyperchaotic system (2) under sliding mode control. The initial conditions are set as $(x_0, y_0, z_0, u_0, v_0) = (0.1, 0.1, 0.1, 0.1, 0.1)$, and the parameters are chosen as $a = 1$, $b = 7$, $c = 9$, $d = 2$, $e = 6$, $m = 3$, and $n = 7$. These values are selected to ensure that the system exhibits hyperchaotic behavior before control is applied, as confirmed in Section 2.

As shown in Fig. 5, the system trajectories successfully converge to zero under the proposed sliding mode control (SMC). Specifically, the state variables z and u reach zero at approximately $t = 0.045$, followed by the variables y and v which are still converging around $t = 0.05$. Finally, the variable x converges at $t = 0.07$. The simulation results confirm that the sliding mode control effectively stabilizes the system's trajectories toward the origin.

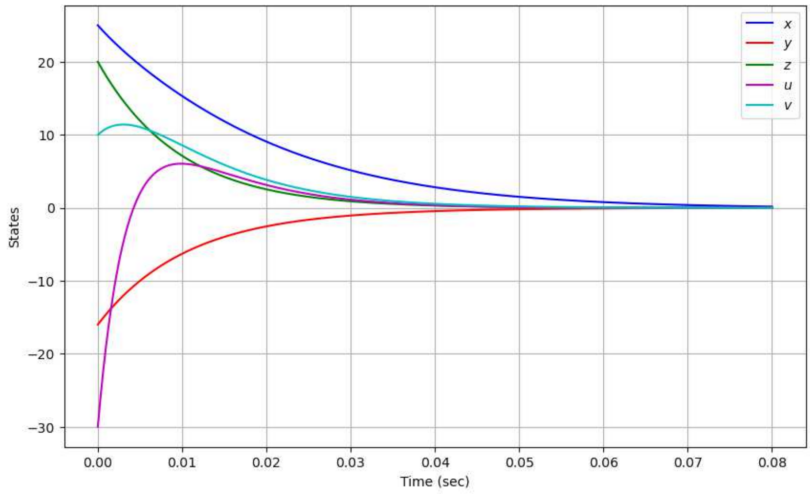

Figure 5: Time responses of the controlled 5D hyperchaotic system (2)

4. Circuit implementation of the novel hyperchaotic system

To design an electronic circuit equivalent to a hyperchaotic system, the process involves three steps, applied as follows:

First step: To establish the appropriate power supply voltage, the temporal trends of the five state variables must be analyzed using MATLAB. Figure 6 illustrates the behavior of these variables and the hyperchaotic attractor, with the ranges defined as:

$$x \in (-300, 300), \quad y \in (-15, 15), \quad z \in (-5, 25), \quad u \in (-300, 300), \quad v \in (-60, 80).$$

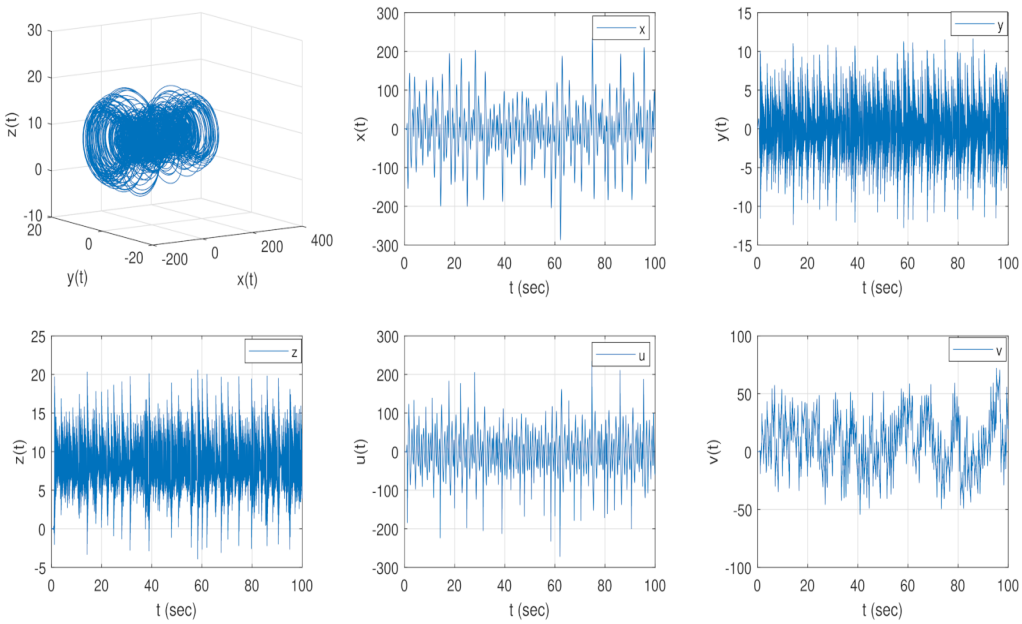

Figure 6: Numerical simulations of the system (2): the hyperchaotic attractor and the trends of the state variables x, y, z, u, and v with $a = 1$, $b = 7$, $c = 9$, $d = 2$, $e = 6$, $m = 3$, $n = 7$, and $(x_0, y_0, z_0, u_0, v_0) = (0.1, 0.1, 0.1, 0.1, 0.1)$

The state variables of the system are scaled to bring the attractor within the dynamic range of the operational amplifiers, where the transformations are givenby:

$$X = \frac{x}{100}, \quad Y = \frac{y}{10}, \quad Z = \frac{z}{10}, \quad U = \frac{u}{100}, \quad V = \frac{v}{10}.$$

A new rescaled equivalent system is established (16), demonstrating that the trends of the state variables oscillate within the voltage limits, as shown in Fig. 7. Thus, the novel hyperchaotic system (2) can be rewritten as:

$$\begin{cases} \dot{X} = a(0.1Y - X) + bU, \\ \dot{Y} = 10cX + dY - 100XZ + V, \\ \dot{Z} = 100XY - eZ, \\ \dot{U} = -mX - 10mY^3, \\ \dot{V} = -10nYZ. \end{cases} \tag{16}$$

Second step: Discuss the circuit associated with the rescaled system, utilizing operational amplifiers to perform the basic operations of addition, subtraction, and integration. The nonlinear terms in the equations are implemented using

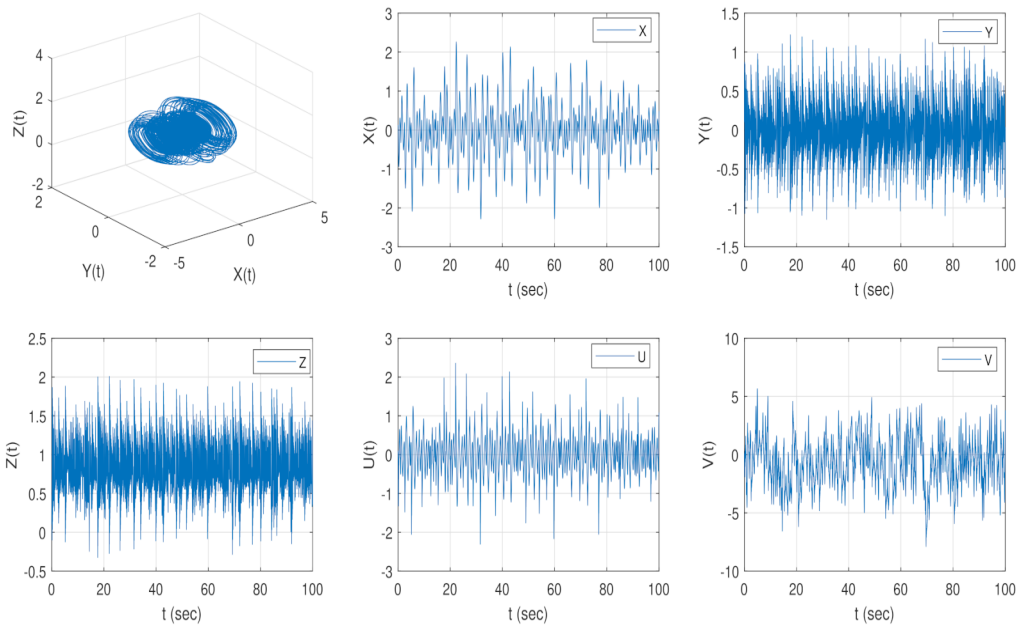

Figure 7: Numerical simulations of the system (16): hyperchoatic attractor and trend of the state variables x, y, z, u, and v with $a = 1$, $b = 7$, $c = 9$, $d = 2$, $e = 6$, $m = 3$, $n = 7$ and $(x_0, y_0, z_0, u_0, v_0) = (0.1, 0.1, 0.1, 0.1, 0.1)$

the analog multipliers AD633, along with other electronic components such as resistors and capacitors. By applying Kirchhoff's laws, the 5D hyperchaotic dynamo system and its circuital equations are derived as:

$$\begin{cases} \dfrac{d\vartheta_{C_1}}{\tau} = \dfrac{1}{C_1}\left(\dfrac{1}{R_1}\vartheta_{C_1} + \dfrac{1}{R_2}\left(\dfrac{R_{11}}{R_{10}}\right)\left(-\vartheta_{C_2}\right) + \dfrac{1}{R_3}\left(\dfrac{R_{17}}{R_{16}}\right)\left(-\vartheta_{C_4}\right)\right), \\ \dfrac{d\vartheta_{C_2}}{\tau} = \dfrac{1}{C_2}\left(\dfrac{1}{R_6}\left(\dfrac{R_4}{R_5}\right)\left(-\vartheta_{C_1}\right) + \dfrac{1}{R_7}\left(\dfrac{R_{11}}{R_{10}}\right)\left(-\vartheta_{C_2}\right) + \dfrac{1}{10R_8}\vartheta_{C_1}\vartheta_{C_3}\right. \\ \qquad\qquad \left. + \dfrac{1}{R_9}\left(\dfrac{R_{20}}{R_{19}}\right)\left(-\vartheta_{C_5}\right)\right), \\ \dfrac{d\vartheta_{C_3}}{\tau} = \dfrac{1}{C_3}\left(\dfrac{1}{10R_{12}}\left(\dfrac{R_4}{R_5}\right)\left(-\vartheta_{C_1}\vartheta_{C_2}\right) + \dfrac{1}{R_{13}}\vartheta_{C_3}\right), \\ \dfrac{d\vartheta_{C_4}}{\tau} = \dfrac{1}{C_4}\left(\dfrac{1}{R_{14}}\vartheta_{C_1} + \dfrac{1}{R_{15}}\vartheta_{C_2}^3\right), \\ \dfrac{d\vartheta_{C_5}}{\tau} = \dfrac{1}{C_5}\left(\dfrac{1}{10R_{18}}\vartheta_{C_2}\vartheta_{C_3}\right), \end{cases} \tag{17}$$

where ϑ_{C_1}, ϑ_{C_2}, ϑ_{C_3}, ϑ_{C_4}, and ϑ_{C_5} are the voltages across the capacitors C_1, C_2, C_3, C_4, and C_5, respectively. By comparing equation (16) with the circuital equation (17), we obtain:

$$\begin{aligned}
a &= \frac{1}{C_1 R_1}, \\
0.1a &= \frac{1}{C_1 R_2}\left(\frac{R_{11}}{R_{10}}\right), \\
b &= \frac{1}{C_1 R_3}\left(\frac{R_{17}}{R_{16}}\right), \\
10c &= \frac{1}{C_2 R_6}\left(\frac{R_5}{R_4}\right), \\
d &= \frac{1}{C_2 R_7}\left(\frac{R_{11}}{R_{10}}\right), \\
100 &= \frac{1}{10 C_2 R_8}, \\
1 &= \frac{1}{C_2 R_9}\left(\frac{R_{20}}{R_{19}}\right), \\
100 &= \frac{1}{10 C_3 R_{12}}\left(\frac{R_5}{R_4}\right), \\
e &= \frac{1}{C_3 R_{13}}, \\
m &= \frac{1}{C_4 R_{14}}, \\
10m &= \frac{1}{C_4 R_{15}}, \\
10n &= \frac{1}{10 C_5 R_{18}},
\end{aligned} \tag{18}$$

Third step: In this final step, the proposed circuit is implemented using Multisim software (version 14.2). The simulation circuit diagram of the system (17) shown in Fig. 8, where the circuital elements are chosen as follows: the power supply voltage is ±9 V; the capacitors are set to $C_1 = C_2 = C_3 = C_4 = C_5 = 1$ nF; and the resistors are $R_4 = R_{10} = R_{16} = R_{19} = 100$ kΩ, and $R_5 = R_{11} = R_{17} = R_{20} = 50$ kΩ. The parameters are chosen as $a = 1$, $b = 7$, $c = 9$, $d = 2$, $e = 6$, $m = 3$, and $n = 7$. The Multisim phase portraits of the 5D hyperchaotic circuit (17) are shown in Fig. 9 corresponding to the simulation presented in the 2D MATLAB plots in Fig. 2, on the planes $x - y$, $x - z$, $x - u$, and $y - u$.

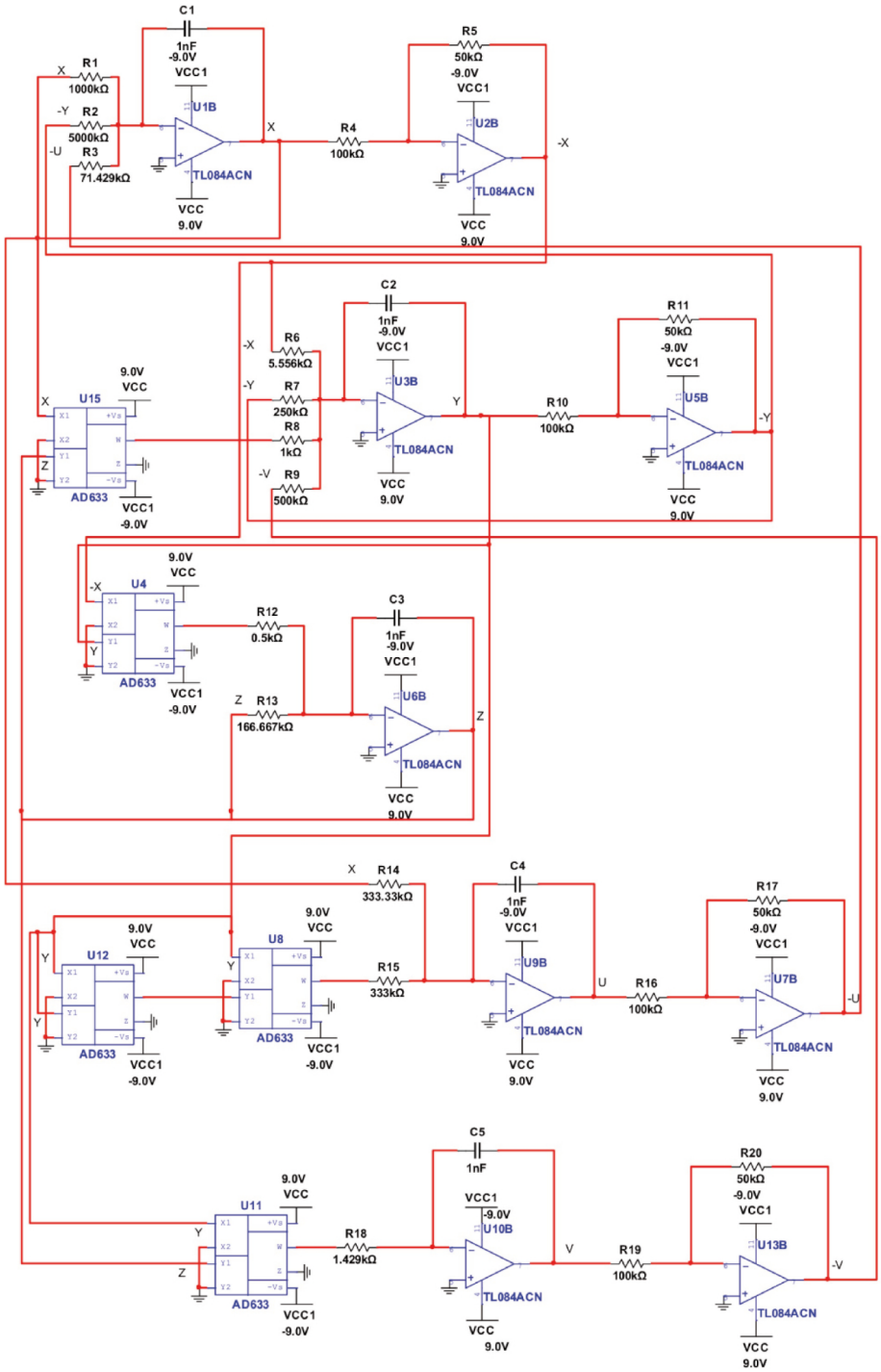

Figure 8: Schematic diagrams of hyperchaotic circuit of circuital equations (17)

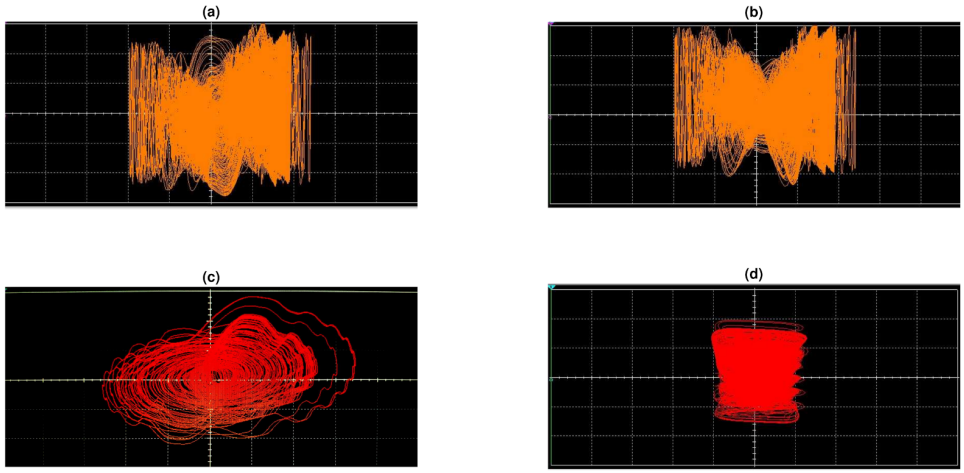

Figure 9: 2-D plots of the 5-D hyperchaotic circuit (17) in (a) $x - y$ plan, (b) $x - z$ plan, (c) $x - u$ plan, (d) $y - u$ plan

5. Conclusion

This paper focuses on the study of a new 5D hyperchaotic system (2) characterized by four nonlinear terms. The complex dynamical behavior of the system is analyzed using phase portraits, Lyapunov exponents, and bifurcation diagrams. The results confirm the existence of a strang attractors and hyperchaotic behavior. Additionally, the system is symmetric with respect to the z-axis, adding an interesting structural property to its dynamics. We have proposed a sliding mode control strategy to stabilize the system at the origin. The method begins by defining an appropriate sliding surface, followed by constructing a controller that drives the system's trajectories toward this surface using an exponential reaching law. The Lyapunov stability criterion is employed to ensure system stability, and Python-based simulations validate the performance of the proposed control approach. Finally, to validate the practical realization of the proposed hyperchaotic system, an electronic circuit was simulated using Multisim software. The circuit results confirm the presence of chaotic behavior, consistent with the theoretical model. Furthermore, the system's attractor is simulated and visualized using MATLAB, demonstrating an excellent correlation between numerical analysis and circuit implementation.

References

[1] E.N. Lorenz: Deterministic nonperiodic flow. *Journal of Atmospheric Sciences*, **20**(2), (1963), 130–141, DOI: 10.1175/1520-0469(1963)020<0130:DNF>2.0.CO;2

[2] J.C. Sprott: Some simple chaotic flows. *Phys. Rev. E*, **50**(2), (1994), 647–650, DOI: 10.1103/PhysRevE.50.R647

[3] Y. Mao, G. Chen and S. Lian: A novel fast image encryption scheme based on 3D chaotic baker maps. *International Journal of Bifurcation and Chaos*, **14**(10), (2004), 3613–3624, DOI: 10.1142/S021812740401151X

[4] G. Dong, R. Du, L. Tian and Q. Jia: A novel 3D autonomous system with different multilayer chaotic attractors. *Physics Letters A*, **373**(42), (2009), 3838–3845, DOI: 10.1016/j.physleta.2009.07.022

[5] J. Kengne, S. Jafari, Z.T. Njitacke, M. Yousefi Azar Khanian and A. Cheukem: Dynamic analysis and electronic circuit implementation of a novel 3D autonomous system without linear terms. *Communications in Nonlinear Science and Numerical Simulation*, **52**, (2017), 62–76, DOI: 10.1016/j.cnsns.2017.04.017

[6] Y. Wu, C. Wang and Q. Deng: A new 3D multi-scroll chaotic system generated with three types of hidden attractors. *Eur. Phys. J. Spec. Top.*, **230**, (2021), 1863–1871, DOI: 10.1140/epjs/s11734-021-00119-8

[7] J.-G. Barajas-Ramírez, A. Franco-Lopez and H.G. Gonzalez-Hernandez: Generating Shilnikov chaos in 3D piecewise linear systems. *J. Appl. Math. Comput.*, **65**(1), (2021), 263–276, DOI: 10.1016/j.amc.2020.125877

[8] S. Vaidyanathan, F. Hannachi, M. A. Mohamed, A. Sambas, C. Aruna and R. Ramesh: A new chaotic hyperjerk system with a half-line of equilibrium points, its dynamic analysis, multistability, circuit simulation and anti-synchronization via backstepping control. *Archives of Control Sciences*, **35**(1), (2025), 123–143, DOI: 10.24425/acs.2025.153960

[9] A. Algaba, F. Fernández-Sánchez, M. Merino and A.J. Rodríguez-Luis: Chen's attractor exists if Lorenz repulsor exists: The Chen system is a special case of the Lorenz system. *Chaos*, **23**(3), (2013), 033108, DOI: 10.1063/1.4813227

[10] L. Meddour and E. Zeraoulia: About the three-dimensional quadratic autonomous system with two quadratic terms equivalent to the Lorenz system. *Dyn. Contin. Discrete Impuls. Syst. B.*, **27**(3b), (2020), 133–143, https://online.watsci.org/abstract_pdf/2020v27/v27n3b-pdf/2.pdf

[11] O.E. Rossler: An equation for hyperchaos. *Phys. Lett. A*, **71**(2-3), (1979), 155–157, DOI: 10.1016/0375-9601(79)90150-6

[12] J. Qiang: Hyperchaos generated from the Lorenz chaotic system and its control. *Phys. Lett. A*, **366**(3), (2007), 217–222, DOI: 10.1016/j.physleta.2007.02.024

[13] Zh. Yan: Controlling hyperchaos in the new hyperchaotic Chen system. *Appl. Math. Comput.*, **168**(2), (2005), 1239–1250, DOI: 10.1016/j.amc.2004.10.016

[14] Y. Li, Z.M. Zhang and Z.J. Tao: A hyperchaotic sixth-order Chua's circuit and its hardware implementation. *Acta Phys. Sin.*, **58**(10), (2009), 6818–6822. DOI: 10.7498/aps.58.6818

[15] A. Chen, J. Lu, J. Lu and S. Yu, Generating hyperchaotic Lü attractor via state feedback control. *Physica A: Statistical Mechanics and its Applications*, **364**, (2006), 103–110, DOI: 10.1016/j.physa.2005.09.039

[16] M. Mechekef, L. Meddour and T. Houmor: Generation of a multiwing hyperchaotic system with a line equilibrium and its control, *J. Comput. Nonlinear Dynam.*, **20**(4), (2025), 041007, DOI: 10.1115/1.4067860

[17] Y. Ghettout, L. Meddour, T. Hamaizia and R. Ouahabi: Dynamic analysis of a new hyperchaotic system with infinite equilibria and its synchronization. *Nonlinear Dynamics and Systems Theory*, **24**(2), (2024), 147–158, URL: https://e-ndst.kiev.ua/v24n2/4(92).pdf

[18] S. Vaidyanathan, C. Volos and V.T. Pham: Hyperchaos, adaptive control and synchronization of a novel 5-D hyperchaotic system with three positive Lyapunov exponents and its spice implementation. *Archives of Control Sciences*, **24**(4), (2014), 409–446, DOI: 10.2478/acsc-2014-0023

[19] A. Lassoued and O. Boubaker: On new chaotic and hyperchaotic systems: A literature survey. *Nonlinear Analysis: Modelling and Control*, **21**(6), (2016), 770–789, DOI: 10.15388/NA.2016.6.3

[20] N. Cui and J. Li: A new 4D hyperchaotic system and its control. *AIMS Mathematics*, **8**(1), (2022), 905–923, DOI: 10.3934/math.2023044

[21] S. Vaidyanathan, et al.: A 5-D multi-stable hyperchaotic two-disk dynamo system with no equilibrium point: Circuit design, FPGA realization and applications to TRNGs and image encryption. *IEEE Access* **4**, (2021), 1–18, DOI: 10.1109/ACCESS.2021.3085483

[22] M. Yan, X. Liu, J. Jie and Y. Hong: Construction and implementation of wide range parameter switchable chaotic system. *Scientific Reports*, **14**(4059), (2024), 1–16, DOI: 10.1038/s41598-024-54458-2

[23] A. Buscarino, L. Fortuna, M. Frasca and G. Sciuto: A Concise Guide to Chaotic Electronic Circuits, Springer, Cham, (2014), DOI: 10.1007/978-3-319-05900-6

[24] Y. Bian and W. Yu: A secure communication method based on 6-D hyperchaos and circuit implementation. *Telecommun. Syst.*, **77**, (2021), 731–751, DOI: 10.1007/s11235-021-00790-1

[25] Y. Huang and X.S. Yang: Hyperchaos and bifurcation in a new class of four-dimensional Hopfield neural networks. *Neurocomputing*, **69**(13), (2006), 1787–1795, DOI: 10.1016/j.neucom.2005.11.001

[26] S. Vaidyanathan and S. Rasappan: Active controller design for global chaos synchronization of hyperchaotic Bao and hyperchaotic Xu systems. *International Journal of Information Technology Convergence and Services*, **1**(6), (2011), 1–14, DOI: 10.5121/ijitcs.2011.1601

[27] R.A. Meskine, S. Kaouache and O.O. Aybar: A new hyperchaotic system with exponential function nonlinearity: Dynamical properties, control hyperchaos and complete synchronization study. *IAENG International Journal of Applied Mathematics*, **54**(7), (2024), 1329–1335, https://www.iaeng.org/IJAM/issues_v54/issue_7/IJAM_54_7_11.pdf

[28] M. Kopp: Hyperchaos, adaptive control, synchronization, and electronic circuit design of a novel 6D hyperchaotic convective dynamo system. *TechRxiv Preprint.*, (2022), 1–32, DOI: 10.36227/techrxiv.19417961.v1

[29] S. Vaidyanathan, C. Volos and V.T. Pham: Hyperchaos, adaptive control and synchronization of a novel 5-D hyperchaotic system with three positive Lyapunov exponents and its spice implementation. *Archives of Control Sciences*, **24**(4), (2014), 409–446, DOI: 10.2478/acsc-2014-0023

[30] S. Singh: Single input sliding mode control for hyperchaotic Lü system with parameter uncertainty. *Int. J. Dynam. Control* **4**, (2015), 504–514, DOI: 10.1007/s40435-015-0167-0

[31] M.D. Johansyah, et al.: Dynamical analysis and sliding mode controller for the new 4D chaotic supply chain model based on the product received by the customer. *Mathematics*, **12**(13), (2024), 1938–21, DOI: 10.3390/math12131938

[32] J. Liu and X. Wang: Advanced Sliding Mode Control for Mechanical Systems: Design, Analysis and MATLAB Simulation. Tsinghua University Press and Springer, Beijing and Heidelberg, (2011), DOI: 10.1007/978-3-642-20907-9

[33] A. Chaudhary and B. Bhushan: Design of a sliding mode controller (SMC) based on reaching law. *International Journal of Computer Applications*, **182**(10), (2018), 45–49, DOI: 10.5120/ijca2018917720

[34] J. Liu: Sliding Mode Control Using MATLAB, Academic Press (2017).

[35] A.-J. Munoz-Vázquez, G. Fernández-Anaya and J.-D. Sánchez-Torres: Fractional integro-differential sliding mode control of a class of distributed-order nonlinear systems. *J. Appl. Math. Comput.*, **68**(4), (2022), 2743–2760, DOI: 10.1007/s12190-021-01632-8

[36] J. Wang, W. Yu, J. Wang, Y. Zhao, J. Zhang and D. Jiang: A new six-dimensional hyperchaotic system and its secure communication circuit implementation. *International Journal of Circuit Theory and Applications*, **47**(5), (2019), 702–717, DOI: 10.1002/cta.2617

[37] M.-A. Murillo-Escobar, C. Cruz-Hernandez, L. Cardoza-Avendano, D. Murillo-Escobar and R.-M. López-Gutiérrez: Multi-biosignal chaotic encryption scheme based on spread spectrum and global diffusion process for e-health. *Biomedical Signal Processing and Control*, **78**, (2022), 104001, DOI: 10.1016/j.bspc.2022.104001

[38] X. Xu, X. Wang and J. Wen: Chaotic circuit and its application in weak signal detection. *International Journal of Bifurcation and Chaos*, **32**(15), (2022), 2250229, DOI: 10.1142/S0218127422502297

[39] S. Zhou, H. Zhang, Y. Zhang, et al.: Novel hyperchaotic image encryption method using machine learning-RBF. *Nonlinear Dynamics*, **112**, (2024), 18527–18550, DOI: 10.1007/s11071-024-09966-1

[40] A.-A. Al-Hussein, F.-R. Tahir and G.-A. Al-Suhail: Design and FPGA implementation of a hyper-chaotic system for real-time secure image transmission. *Iraqi Journal for Electrical and Electronic Engineering*, **21**(1), (2024), 55–68, DOI: 10.37917/ijeee.21.1.6

[41] J. Luo, S. Qu, Y. Chen, X. Chen and Z. Xiong: Synchronization, circuit and secure communication implementation of a memristor-based hyperchaotic system using single input controller. *Chinese Journal of Physics*, **71**, (2021), 403–417, DOI: 10.1016/j.cjph.2021.03.009

[42] X. Chen, et al., Pseudorandom number generator based on three kinds of four-wing memristive hyperchaotic system and its application in image encryption. *Complexity*, **2020**(1), (2020), 8274685, DOI: 10.1155/2020/8274685

[43] G. Li and B. Zhang: A novel weak signal detection method via chaotic synchronization using Chua's circuit. *IEEE Transactions on Industrial Electronics*, **64**(3), (2016), 2255–2265, DOI: 10.1109/TIE.2016.2620103

[44] S. Celikovský and G. Chen: On a generalized Lorenz canonical form of chaotic systems. *Int. J. Bifurc. Chaos*, **12**(8), (2002), 1789–1812, DOI: 10.1142/S0218127402005467